

The Asparagine-Rich Protein NRP Facilitates the Degradation of the PP6-type Phosphatase FyPP3 to Promote ABA Response in *Arabidopsis*

Tong Zhu¹, Yanying Wu¹, Xiaotong Yang¹, Wenli Chen¹, Qingqiu Gong^{2,*} and Xinqi Liu^{1,*}

¹State Key Laboratory of Medicinal Chemical Biology, Department of Biochemistry and Molecular Biology, College of Life Sciences, Nankai University, Tianjin 300071, China

²Tianjin Key Laboratory of Protein Science, Department of Plant Biology and Ecology, College of Life Sciences, Nankai University, Tianjin 300071, China

*Correspondence: Qingqiu Gong (gongq@nankai.edu.cn), Xinqi Liu (liu2008@nankai.edu.cn)

<https://doi.org/10.1016/j.molp.2017.11.006>

ABSTRACT

The phytohormone abscisic acid (ABA) plays critical roles in abiotic stress responses and plant development. In germinating seeds, the phytochrome-associated protein phosphatase, FyPP3, negatively regulates ABA signaling by dephosphorylating the transcription factor ABI5. However, whether and how FyPP3 is regulated at the posttranscriptional level remains unclear. Here, we report that an asparagine-rich protein, NRP, interacts with FyPP3 and tethers FyPP3 to SYP41/61-positive endosomes for subsequent degradation in the vacuole. Upon ABA treatment, the expression of NRP was induced and NRP-mediated FyPP3 turnover was accelerated. Consistently, ABA-induced FyPP3 turnover was abolished in an *nrp* null mutant. On the other hand, FyPP3 can dephosphorylate NRP *in vitro*, and overexpression of FyPP3 reduced the half-life of NRP *in vivo*. Genetic analyses showed that NRP has a positive role in ABA-mediated seed germination and gene expression, and that NRP is epistatic to FyPP3. Taken together, our results identify a new regulatory circuit in the ABA signaling network, which links the intracellular trafficking with ABA signaling.

Key Words: protein interaction, vacuolar degradation, ABA response, germination

Zhu T., Wu Y., Yang X., Chen W., Gong Q., and Liu X. (2018). The Asparagine-Rich Protein NRP Facilitates the Degradation of the PP6-type Phosphatase FyPP3 to Promote ABA Response in *Arabidopsis*. *Mol. Plant*. **11**, 257–268.

INTRODUCTION

The phytohormone abscisic acid (ABA) is a master regulator in abiotic stress adaptation (Finkelstein et al., 2008; Cutler et al., 2010; Fujita et al., 2011; Finkelstein, 2013). Salt, drought, and low temperature can all lead to osmotic stress, which triggers ABA biosynthesis in the vascular parenchyma and in guard cells (Endo et al., 2008; Bauer et al., 2013). ABA also regulates many aspects of plant growth and development, such as seed maturation, dormancy, germination, and seedling growth, as well as vegetative growth, flowering, and leaf senescence (Chiwocha et al., 2005; Finkelstein, 2006, 2013). ABA is perceived through the PYRABACTIN RESISTANT1 (PYR1) and PYR-like (PYLs)/REGULATORY COMPONENT OF ABA RECEPTORS (RCAR) receptors and the ABI-clade Protein Phosphatase 2C (PP2C) co-receptors (Ma et al., 2009; Park et al., 2009). In the core ABA signaling pathway, ABA binds to a PYR/PYL/RCAR to induce a conformational change that stabilizes the interaction between the ABA receptor and a PP2C, leading to inactivation of the PP2C and the derepression of SNF1-related protein kinases (SnRK2s). The SnRK2s can

then phosphorylate and activate numerous downstream signaling components, such as transcription factors, ion channels, and NADPH oxidases, to achieve abiotic stress tolerance (Umezawa et al., 2010; Hauser et al., 2011; Qin et al., 2011).

One transcription factor that can be phosphorylated by SnRK2s is ABA-insensitive 5 (ABI5), a basic leucine zipper (bZIP) transcription factor that was first identified genetically in a screen for mutants insensitive to ABA during germination (Finkelstein and Lynch, 2000), and later established as a central component in ABA-mediated growth repression (Lopez-Molina et al., 2001; Bensmihen et al., 2002; Brocard et al., 2002). ABA-responsive element (ABRE) core motif (CACTGT) is bound by ABI5 as a requisite to activate transcription has been shown *in vitro* and *in vivo* (Lopez-Molina et al., 2001; Carles et al., 2002; Finkelstein et al., 2005; Furihata et al., 2006; Lee et al., 2012). ABI5 expression can be highly induced by ABA during germination or

by ABA and stresses during vegetative growth (Brocard et al., 2002). Furthermore, an orchestration of post-translational modifications has been shown to regulate the activity and stability of ABI5 (Yu et al., 2015). First, three ABA-activated SnRK2s, SRK2D/SnRK2.2, SRK2E/SnRK2.6/OST1, and SRK2I/SnRK2.3, are required for ABI5 phosphorylation (Nakashima et al., 2009). Second, dephosphorylation of ABI5 by two homologous Ser/Thr Protein Phosphatase 6 (PP6) catalytic subunits, FyPP1 and FyPP3, was also demonstrated (Dai et al., 2013). FyPP1 and FyPP3 interact with ABI5 *in vitro* and *in vivo*, and dephosphorylate ABI5 *in vitro*. Reduced *FyPP1/FyPP3* expression led to ABA hypersensitivity in germination and seedling growth, and the FyPP protein levels were regulated negatively by ABA. The FyPPs were further demonstrated to act antagonistically with SnRK2s to regulate ABI5 phosphorylation and stability (Dai et al., 2013). In addition, a PP2A-associated protein, TAP46, along with PP2A, has been shown to interact with ABI5 *in vivo*, and binding of TAP46 to ABI5 stabilizes ABI5 and enhances its activity (Hu et al., 2014). Furthermore, the protein level of ABI5 is regulated by an E3 ligase, KEEP ON GOING (KEG) (Stone et al., 2006; Liu and Stone, 2013), a negative regulator of ABA signaling. KEG interacts and ubiquitinates ABI5 *in vitro* and mediates degradation of cytoplasmic ABI5 *in vivo* (Liu and Stone, 2013), whereas ABA suppresses ABI5 degradation by inducing self-ubiquitination and degradation of KEG (Liu and Stone, 2010). S-Nitrosylation of ABI5 promotes its KEG-mediated degradation (Albertos et al., 2015), which explains the antagonistic role of nitric oxide against ABA during seed germination. Interestingly, KEG-mediated ABI5 degradation takes place in the cytoplasm and *trans*-Golgi network (TGN)/early endosome (EE) (Liu and Stone, 2013). By contrast, ABI5 turnover in the nucleus is mediated by *DWD hypersensitive to ABA1 and 2* (*DWA1* and *DWA2*), which are substrate receptors for CULLIN4-RING E3 ligases (Lee et al., 2010). Finally, ABI5 can be sumoylated by the SUMO E3 ligase SIZ1 and protected from ubiquitination (Miura et al., 2009).

One emerging layer of ABA signaling regulation is intracellular trafficking. As described above, ABI5 nuclear-cytoplasmic partitioning is regulated by its turnover through the E3 ligase KEG at the TGN/EE (Liu and Stone, 2013). Other signaling components, such as the FyPPs, are also reported to be localized at the plasma membrane and at intracellular punctate structures (Dai et al., 2012). The *PYR/PYL* ABA receptors interact transiently with the plasma membrane (PM) in a calcium-dependent manner, and their interaction with the C2-domain ABA-related (CAR) proteins significantly enhanced the PM localization (Rodriguez et al., 2014). In addition, *PYR1/PYL4* can be endocytosed in a clathrin-dependent fashion and bound by FYVE1/FREE1 and VPS23A, which are two endosomal sorting complex required for transport (ESCRT) components, for vacuolar degradation (Belda-Palazon et al., 2016; Yu et al., 2016).

In addition to the direct evidence mentioned above, studies have suggested connections between ABA signaling and intracellular trafficking. For instance, *osmotic stress-sensitive 1* (*osm1*) was identified using a screen for abiotic stress-sensitive mutants and had an ABA-insensitive phenotype. *OSM1* encodes SYP61, a soluble *N*-ethylmaleimide-sensitive factor activating protein receptor (SNARE) protein that localizes to the TGN (Sanderfoot et al., 2001). A recent proteomic study on the SYP61 TGN compartment

showed that syntaxin not only forms a complex with the Qa-SNARE proteins SYP41 and SYP43, the Qb-SNARE VTI12, and the regulatory protein VPS45, but also interacts with Rab guanine triphosphatases (GTPases), the transport protein particle (TRAPPI and TRAPPII) complex components, vacuolar sorting receptors, and proteins functioning in exocytosis (Drakakaki et al., 2012). SYP61 interacts with SYP121 to promote the delivery of the aquaporin PIP2;7 to the PM, thus contributing to the regulation of water permeability of the PM (Drakakaki et al., 2012). Clearly, the essential components of ABA signaling network not only are fine-tuned by exquisite post-translational modifications, but their subcellular localization and levels are also adjusted precisely by multiple intracellular trafficking routes.

The asparagine-rich protein NRP was first characterized as a marker for the soybean hypersensitive response: it was strongly induced during *Pseudomonas syringae* pv. *glycinea* infection (Ludwig and Tenhaken, 2001). Homologs of GmNRPs were then identified in higher plants. NRPs generally have an N-terminal domain rich in asparagine (~25%), and a significantly conserved, plant-specific C-terminal domain termed the developmental and cell death (DCD) domain. The DCD domain is approximately 130 amino acids long, with N-terminal FGLP and LFL motifs, and C-terminal PAQV and PLxE motifs (Tenhaken et al., 2005). Transient expression of the soybean NRP-A and NRP-B promoted a caspase-3-like activity to induce programmed cell death (PCD) in soybean protoplasts and senescence in tobacco leaves (Costa et al., 2008). This specific death signal can be delayed by overexpressing the ER chaperone BiP (Reis et al., 2011). The *Arabidopsis* NRP is also stress responsive, and can induce cell death when overexpressed in tobacco leaves. Furthermore, the *nrp* mutant exhibited hypersensitive phenotypes upon salt and osmotic stresses, and was less sensitive to tunicamycin-induced ER stress (Hoepflinger et al., 2011; Reis et al., 2016). NRP was revealed not only to be decreased by the existence of BiP in *Arabidopsis*, but also to act as a “signaling center” for other related genes to work continuously during osmotic stress (Reis et al., 2011). Although downstream components have been described for NRP-mediated PCD (Reis et al., 2016), the precise function of NRP in salt and osmotic stresses remains unclear.

In this report, we show that the stress protein NRP is a new component of ABA signaling. By interacting with the PP6 FyPP3, NRP recruits FyPP3 to the endosome, and promotes the turnover of FyPP3. Such degradation is likely to occur in the vacuole. Exogenous ABA promotes NRP transcription, leading to accelerated degradation of FyPP3. Overexpression of NRP confers sensitivity toward ABA, and the *nrp* mutant is less ABA sensitive. We also show that FyPP3 is able to dephosphorylate NRP *in vitro*, and that overexpression of FyPP3 shortens the half-life of NRP *in vivo*.

RESULTS

NRP Interacts with FyPP3 Both *In Vitro* and *In Vivo*

To explore the possible roles of NRP in abiotic stress adaptation, we performed a yeast two-hybrid screen using NRP as bait. FyPP3 was identified as an NRP-interacting partner (Figure 1A and Supplemental Table 1). To confirm the interaction, we performed *in vitro* pull-down assays (Figure 1B). When

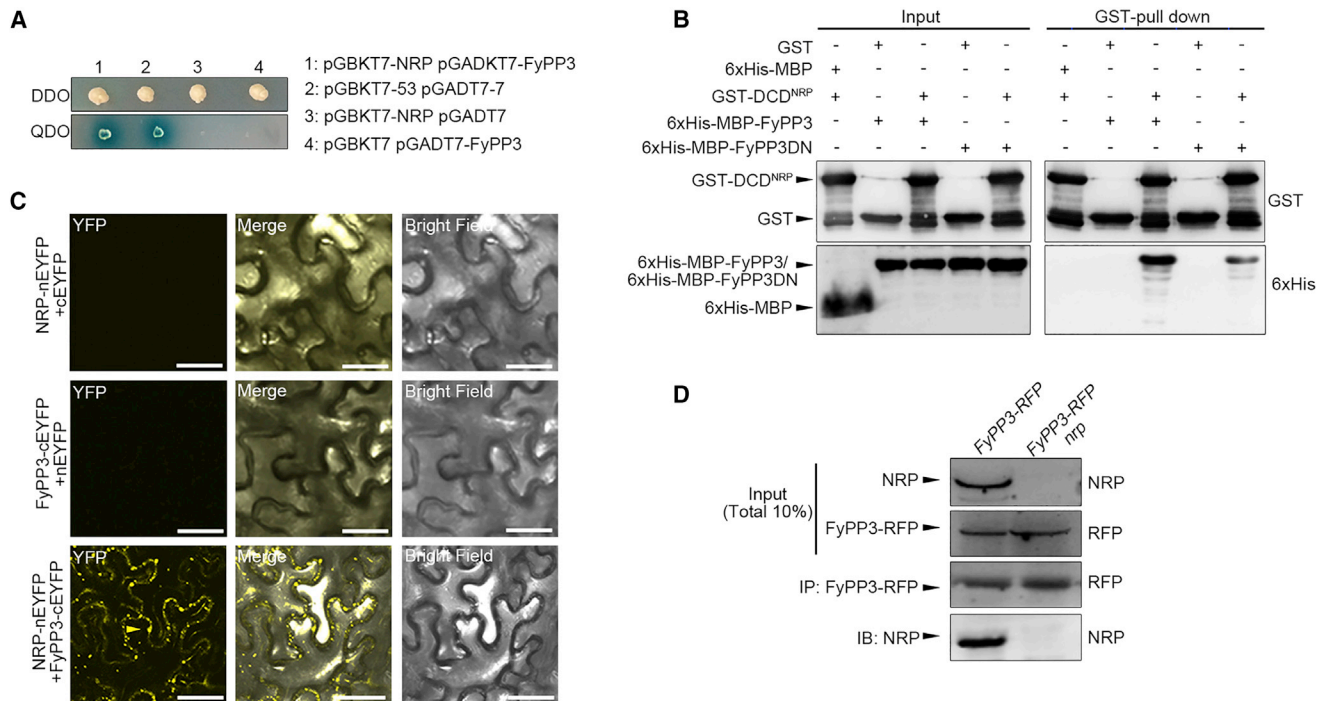


Figure 1. Interaction between NRP and FyPP3 *In Vitro* and *In Vivo*.

(A) NRP interacts with FyPP3 in a yeast two-hybrid assay. NRP translationally fused with the Gal4 DNA-binding domain (pGBKT7-NRP) can interact with FyPP3 fused with the Gal4 activation domain (pGADKT7-FyPP3). pGBKT7-53 and pGADT7-7 is a pair of positive controls. DDO, medium without Trp and Leu; QDO, medium without Trp, Leu, His, and Ade. X- α -gal was added in QDO.

(B) NRP interacts with FyPP3 in a GST pull-down assay. Prokaryotically expressed/purified 6 \times His-MBP-tagged FyPP3 (6 \times His-MBP-FyPP3) and GST-tagged DCD domain of NRP (GST-DCD^{NRP}) were mixed and incubated with anti-GST Sepharose beads, and immunoblotting was done with anti-6 \times His and anti-GST antibodies.

(C) NRP interacts with FyPP3 in tobacco leaves as indicated by the BiFC assay. NRP translationally fused with the C terminus of EYFP (NRP-nEYFP) was co-expressed with FyPP3 translationally fused with the N terminus of EYFP (FyPP3-cEYFP) by co-infiltrating *Agrobacterium* carrying the indicated plasmids into *Nicotiana benthamiana* leaves. Images were collected 2 days after *Agrobacterium* infiltration. Arrowheads indicate representative YFP puncta observed. Scale bar, 25 μ m.

(D) NRP interacts with FyPP3 in a coIP assay. CoIP assay was performed with FyPP3-RFP weak overexpression plants (FyPP3 mRNA level about 1.4-fold that in WT), and FyPP3-RFP *nrp* plants were used as a negative control. Anti-RFP antibody was incubated with Protein A beads to isolate FyPP3-RFP and endogenous NRP. Immunoblotting analysis was done with anti-RFP and anti-NRP antibodies.

expressed in *Escherichia coli*, the full-length NRP was insoluble and unstable, hence its DCD domain was used for glutathione S-transferase (GST) fusion instead. 6 \times His-MBP-tagged FyPP3 (6 \times His-MBP-FyPP3) was able to recover the GST-tagged DCD domain of NRP (GST-DCD^{NRP}), with a stoichiometry of about 1:1 (Figure 1B). The recovery of GST-DCD^{NRP} was reduced significantly when the phosphatase-dead FyPP3 (FyPP3DN, dominant-negative FyPP3 harboring a D81N mutation) (Dai et al., 2013) was used in the input (Figure 1B), indicating that the phosphatase activity of FyPP3 is required for the interaction *in vitro*.

The interaction between FyPP3 and NRP was further confirmed using bimolecular fluorescence complementation (BiFC) in tobacco leaf epidermal cells. When NRP-nEYFP and FyPP3-cEYFP were co-expressed, yellow fluorescent protein (YFP) signals were detected at both the PM and punctate structures in the cytoplasm (Figure 1C).

To validate the FyPP3-NRP interaction *in vivo*, we tried to raise polyclonal antibodies toward the two proteins for co-immunoprecipitation (coIP) assay. Only anti-NRP was successfully

produced. Hence, proteins extracted from an *Arabidopsis* transgenic line carrying FyPP3-RFP, with its FyPP3 mRNA level moderately higher (1.4-fold) than the wild-type (WT) (L2-1 in Supplemental Figure 1C), was used for coIP. The results indicated that native NRP could co-immunoprecipitate with FyPP3-RFP (Figure 1D). FyPP3-RFP *nrp* was used as a negative control.

NRP Tethers FyPP3 to SYP41/SYP61-Positive Endosomes

To uncover the nature of the intracellular puncta observed in BiFC (Figure 1C), we carried out co-localization studies in both transiently transformed tobacco leaf epidermal cells and *Arabidopsis* transgenic lines (Figure 2A and 2B). Transient and stable expression gave consistent results, whereby NRP-GFP and FyPP3-RFP were detected at the PM and in intracellular puncta (Figure 2A and 2B). Since FyPP3 and NRP puncta do not always co-localize, we calculated the percentage of NRP-GFP puncta that co-localize with FyPP3-RFP and the percentage of FyPP3-RFP puncta that co-localize with NRP-GFP separately (Figure 2C and 2D). It turns out that 88% \pm 9% of the FyPP3 puncta co-localize with NRP, whereas 36% \pm 7% of NRP

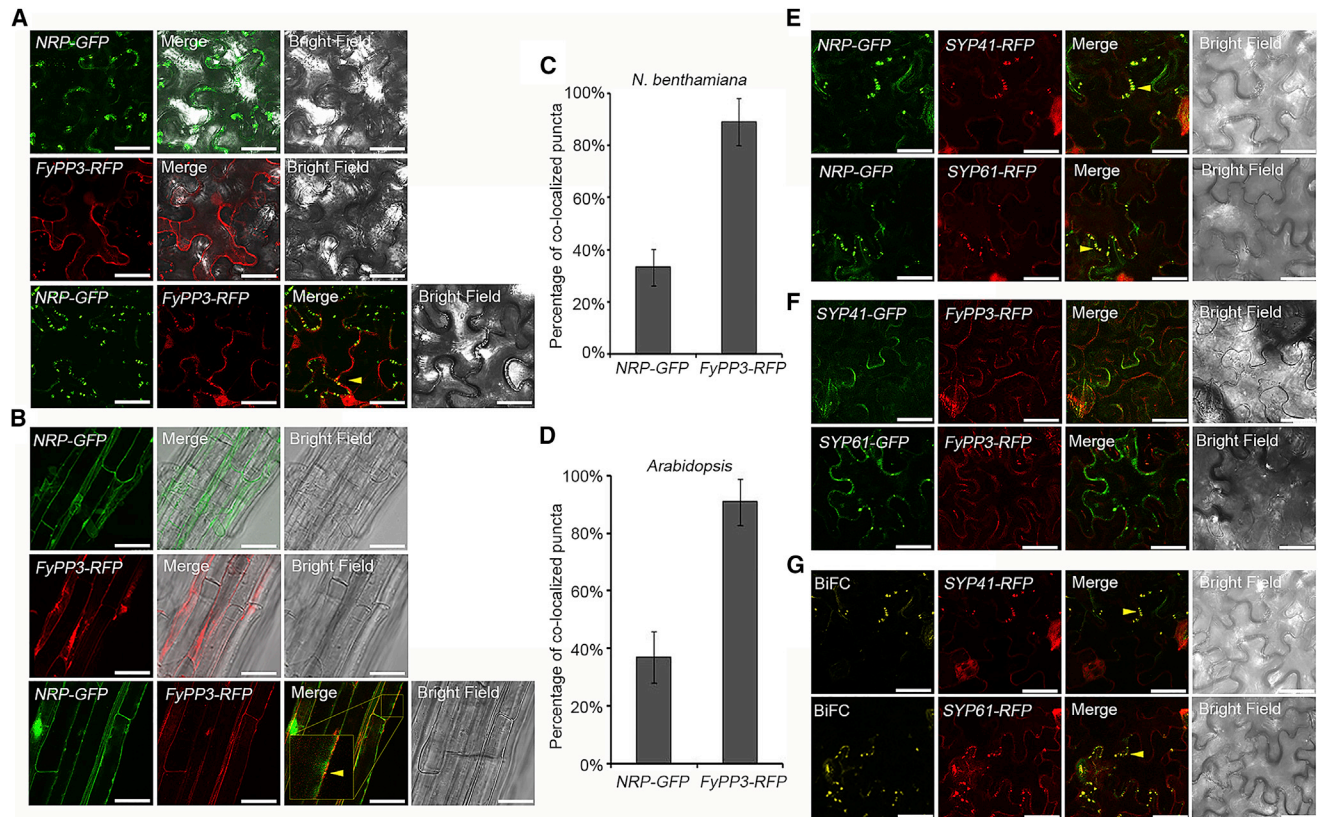


Figure 2. Subcellular Locations of NRP and FyPP3.

All constructs were driven by the *CaMV 35S* promoter. Arrowheads indicate co-localization in merged images.

(A) Co-localization of NRP and FyPP3 in tobacco leaf epidermal cells. *NRP-GFP* and *FyPP3-RFP* were transiently co-expressed in *N. benthamiana* leaves. NRP and FyPP3 co-localize to punctate structures in the cytoplasm.

(B) Co-localization of NRP and FyPP3 in *Arabidopsis* root epidermal cells. The roots of transgenic lines carrying *NRP-GFP*, *FyPP3-RFP*, and the double transgenic line were analyzed.

(C) Quantification of co-localized puncta in **(A)**. Percentage of *NRP-GFP* puncta that co-localize with *FyPP3-RFP*, and percentage of *FyPP3-RFP* puncta that co-localize with *NRP-GFP* are calculated separately and shown (>200 puncta each from >30 cells). Error bars denote SD.

(D) Percentage of co-localized puncta in **(B)**. Percentages were calculated as in **(C)**. Error bars denote SD.

(E) Co-localization of GFP-tagged NRP (*NRP-GFP*) and RFP-tagged endosomal markers, SYP41 and SYP61, in transiently co-transformed tobacco leaf epidermal cells.

(F) Co-localization of RFP-tagged FyPP3 (*FyPP3-RFP*) and GFP-tagged SYP41 and SYP61 in tobacco leaves.

(G) The interaction between NRP and FyPP3 takes place at SYP41/SYP61-positive endosomes. BiFC assay was carried out for NRP and FyPP3 as in **Figure 1C**, with co-transformed SYP41-RFP or SYP61-RFP in tobacco leaves.

All scale bars represent 25 μ m.

overlaps with FyPP3. To identify the puncta, we co-expressed *NRP-GFP* and *FyPP3-RFP* with various organelle markers, and two TGN/EE markers, SYP41 and SYP61, clearly co-localized with NRP (**Figure 2E** and **Supplemental Figure 2**). In contrast, no obvious puncta could be observed in the cells overexpressing FyPP3 alone (**Figure 2A**, **2B**, and **2F**), suggesting that the interaction between NRP and FyPP3 could tether the latter to SYP41/61-positive endosomes. Indeed, when *NRP-nEYFP* and *FyPP3-cEYFP* were co-transformed with either *SYP41-RFP* or *SYP61-RFP*, it was clearly seen that the NRP-FyPP3 interaction takes place at the TGN/EE (**Figure 2G**).

NRP-FyPP3 Interaction Accelerates Mutual Degradation Following ABA Treatment

Since FyPP3 can be recruited by NRP to SYP41/61-positive TGN/EE vesicles, we wanted to see if the two are subsequently

degraded in the vacuole, and whether this process can be regulated by ABA. We firstly obtained an *nrp* null mutant, and generated RNA interference lines that simultaneously reduce the mRNA level of FyPP3 and its homolog FyPP1 (Xu et al., 2010). The T3 homozygous RNAi lines were analyzed for their FyPP3 and FyPP1 transcript levels (**Supplemental Figure 1A**), and a strong RNAi line, L3-2, was used. To test whether the phosphatase activity of FyPP3 is required for the stability of both FyPP3 and NRP, we also generated *FyPP3DN* lines (**Supplemental Figure 1E**). The double transgenic lines *FyPP3-RFP NRP-GFP*, *FyPP3DN-RFP NRP-GFP*, and *FyPP3-RFP nrp* were then generated to study the relationship between the two. We first analyzed the tissue-specific expression of *NRP* and *FyPP3* by qRT-PCR. Both genes are ubiquitously expressed and are correlated in distribution (**Supplemental Figure 3**).

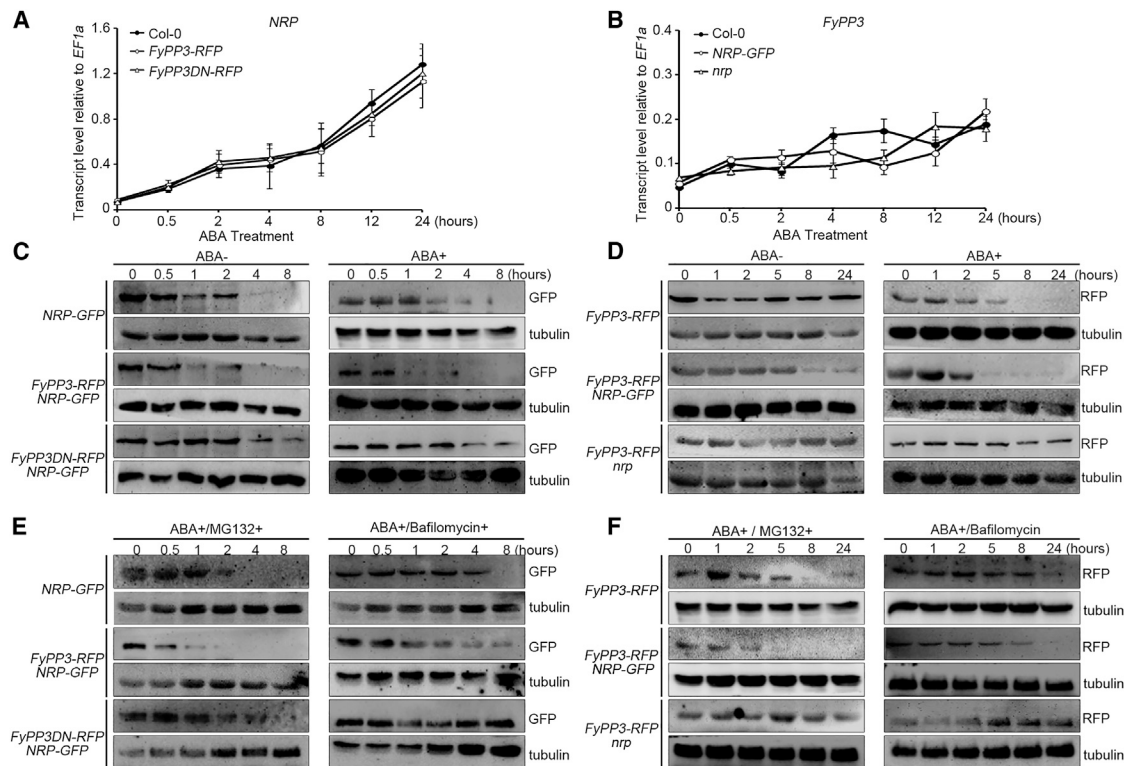


Figure 3. ABA-Induced FyPP3 Turnover Is Facilitated by NRP.

(A and B) The transcript levels of *NRP* and *FyPP3* in different lines following treatment with 5 μ M ABA. **(A)** ABA treatment induces *NRP* expression in the WT (Col-0), *FyPP3* overexpression (*FyPP3-RFP*), and *FyPP3* dominant-negative (*FyPP3DN-RFP*) lines to similar levels over a 24-h time course. **(B)** The transcript level of *FyPP3* is slightly induced by ABA treatment, and is not affected by the level of *NRP*. *EF1a* was used as an internal control. Three biological replicates, each composed of four technical replicates were done for both **(A)** and **(B)**. Error bars denote SD.

(C) The protein level of NRP in *NRP-GFP*, *FyPP3-RFP NRP-GFP*, and *FyPP3DN-RFP NRP-GFP* seedlings with or without ABA treatment. After 5.5 h of cycloheximide (CHX) treatment, seedlings were immersed in 2 μ M ABA or double-distilled water. The seedlings were collected at 0, 0.5, 1, 2, 4, and 8 h following ABA treatment for protein extraction. Immunoblotting was done with anti-GFP antibody to detect NRP-GFP.

(D) The protein level of FyPP3 in *FyPP3-RFP*, *FyPP3-RFP NRP-GFP*, and *FyPP3-RFP nrp* seedlings with or without ABA. Seedlings were treated as in **(C)**. Immunoblotting was done with anti-RFP antibody to detect FyPP3.

(E) The protein level of NRP in *NRP-GFP*, *FyPP3-RFP NRP-GFP*, and *FyPP3DN-RFP NRP-GFP* with MG132 or bafilomycin (BLA) under ABA treatment. The seedlings were treated with 2 μ M ABA plus 2 μ M MG132 or 40 nM BLA and collected at the indicated time points. Anti-GFP antibody was used for detecting NRP.

(F) The protein level of FyPP3 in *FyPP3-RFP*, *FyPP3-RFP NRP-GFP*, and *FyPP3-RFP nrp* with MG132 or BLA under ABA treatment. Seedlings were treated and collected as in **(E)**. Anti-RFP antibody was used for detecting FyPP3.

Tubulin was used as the loading control in **(C)** to **(F)**.

To further validate the co-expression of *NRP* and *FyPP3*, we generated transcriptional fusions for both genes with GFP as the reporter. In both *ProNRP:GFP* and *ProFyPP3:GFP* transgenic lines, GFP signals were detected in the cotyledons and the radicle of germinating seeds, but not in the seed coat (Supplemental Figure 4A–4D). In the 7-day-old seedlings, GFP was detected in the cotyledons, the primary root, and the vasculature (Supplemental Figure 4E–4G). In 6-week-old plants, both *NRP* and *FyPP3* promoter activities were observed mainly in the vascular tissues, with *FyPP3* promoter activity higher than that of *NRP* at the reproductive stage (Supplemental Figure 4H–4N).

We then examined whether the expressions of *NRP* and *FyPP3* are responsive to exogenous ABA. Indeed, both genes are ABA inducible in WT seedlings, with *NRP* upregulated to a significantly higher level by ABA (Figure 3A and 3B; Supplemental Figure 5). The same trends were observed in all transgenic

lines examined (Figure 3A and 3B). We speculated that the ABA-induced *NRP* expression may be involved in the regulation of *FyPP3*, and that such regulation is likely post-transcriptional.

To examine whether *NRP* and *FyPP3* protein levels can be modulated by each other, and whether ABA may be involved in such regulation, we analyzed turnover rates of both proteins in the transgenic lines and double transgenic lines with or without ABA treatment. Both proteins degraded faster following ABA treatment (Figure 3C and 3D, upper lanes), and both proteins degraded faster when they were co-expressed (Figure 3C and 3D, middle lanes). By contrast, both proteins degraded slower in the absence (*nrp*) or dysfunction (*FyPP3DN*) of the other (Figure 3C and 3D, bottom lanes). To investigate whether the degradation is proteasome-dependent or vacuole-dependent, we repeated the ABA treatment in the presence of MG132 and bafilomycin (BLA), respectively. ABA-induced degradation of

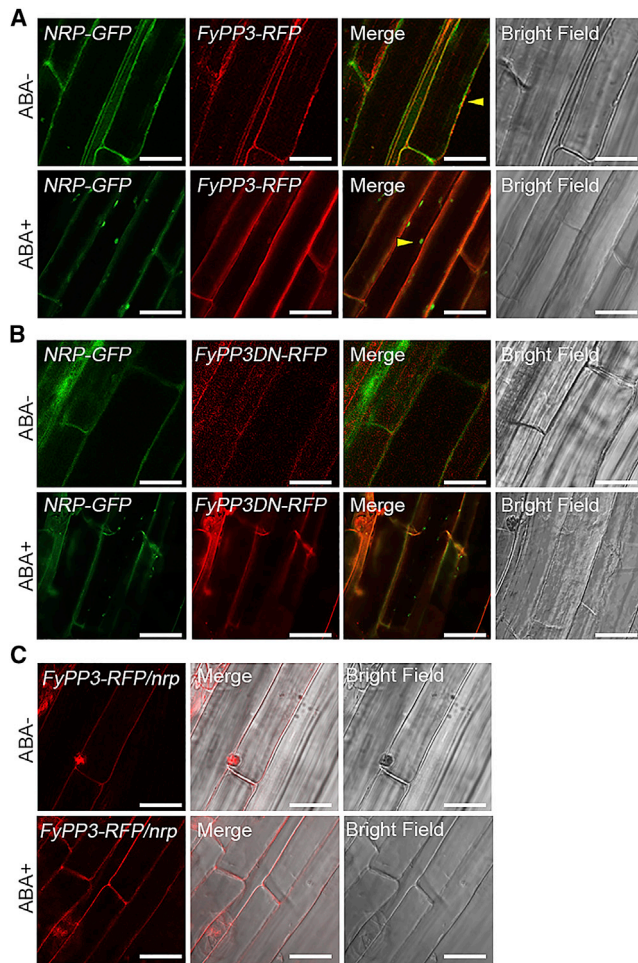


Figure 4. Subcellular Localization Patterns of NRP and FyPP3 with or without ABA.

(A) Co-localization of NRP-GFP and FyPP3-RFP upon 2 μ M ABA treatment in the root epidermal cells of *FyPP3-RFP NRP-GFP* seedlings. Seven-day-old seedlings were immersed in water (ABA⁻) or 2 μ M ABA (ABA⁺) for 1 h. Arrowheads indicate co-localization between the two proteins.

(B) Co-localization of NRP-GFP and FyPP3DN-RFP following ABA treatment in *FyPP3DN-RFP NRP-GFP* seedlings. Seedlings were treated as in **(A)**.

(C) Localization of FyPP3 in *FyPP3-RFP nrp* seedlings following ABA treatment. Seedlings were treated as in **(A)**. All scale bars represent 10 μ m.

NRP and FyPP3 was attenuated by bafilomycin, but not MG132, indicating that the vacuole is involved in the degradation of both proteins (Figure 3E and 3F).

Since we observed co-localization of NRP and FyPP3 (Figure 2A and 2B) and their ABA-induced degradation (Figure 3C and 3D), we speculated that their co-localization might increase following ABA treatment. Indeed, ABA induced the formation of large puncta in the *NRP-GFP FyPP3-RFP* double transgenic line, but not in *NRP-GFP FyPP3DN-RFP* (Figure 4A and 4B). These enlarged puncta were reminiscent of large protein aggregates that are marked for degradation. As expected, no puncta were observed in *FyPP3-RFP nrp* with or without ABA (Figure 4C).

FyPP3 Dephosphorylates NRP Efficiently *In Vitro*

FyPP3 has been shown to dephosphorylate PIN1, PhyA, and ABI5 to regulate their functions (Kim et al., 2002; Dai et al., 2012). NRP has multiple potential Ser/Thr phosphorylation sites within its sequence as predicted by an online server, NetPhos (<http://www.cbs.dtu.dk/services/NetPhos/>). The fact that FyPP3DN and FyPP3 act oppositely in NRP turnover (Figure 3C–3F) suggested that NRP could be a substrate of FyPP3. To address this, we carried out a dephosphorylation assay. Equal aliquots of GST-DCD^{NRP} expressed/purified from *E. coli* were incubated with Columbia-0 (Col-0), *FyPP3-RFP*, and *FyPP3DN-RFP* homogenates with Zn²⁺, respectively. Since purified GST-DCD^{NRP} was already phosphorylated by some unknown kinase in *E. coli* (Figure 5A), alkaline phosphatase (AP) was used to eliminate the phosphorylation in GST-DCD^{NRP}. As expected, the amount of phosphorylated GST-DCD^{NRP} was significantly decreased when GST-DCD^{NRP} was incubated with the *FyPP3-RFP* homogenate, but not with the *FyPP3DN-RFP* homogenate (Figure 5A). Therefore, FyPP3 can efficiently dephosphorylate NRP *in vitro*. Furthermore, the *in vitro* interaction between NRP and FyPP3 is indeed dependent on the phosphorylation status of NRP (Figure 5B). We speculated that, like ABI5, phosphorylated NRP might function as an active form to regulate the transportation and degradation of targeted proteins, and that dephosphorylation of NRP by FyPP3 might lead to its inactivation.

NRP and FyPP3 Function in ABA-Regulated Seed Germination

ABA is a key factor in controlling seed germination and seedling growth. To address the possible roles of NRP and FyPP3 in ABA-regulated germination, we first confirmed that the promoter activities of both genes were responsive to exogenous ABA in the germinating seeds (Supplemental Figure 4C and 4D). We then carried out a germination assay on the eight transgenic lines (knockout or loss-of-function, overexpression, and double transgenic lines) along with the WT (Col-0) with concentrations of ABA spanning from 0 to 5 μ M (Figure 6A). Compared with the WT, overexpression of NRP led to ABA-sensitive phenotypes, whereas the *nrp* seeds were moderately ABA insensitive (Figure 6B). As reported before, *FyPP3/FyPP1 RNAi* and *FyPP3DN* showed more sensitivity to ABA, whereas FyPP3 overexpression decreased the sensitivity (Dai et al., 2013) (Figure 6B). *FyPP3-RFP nrp* showed higher resistance than *FyPP3* or *nrp* alone at higher concentrations of ABA. Furthermore, co-expression of NRP and FyPP3 led to a phenotype similar to that of the WT, indicating that NRP mitigates the function of FyPP3 (Figure 6B).

We also checked the expression of several ABA-responsive genes, *RD29B*, *RAB18*, and *MYC2*, in the nine lines. Consistent with the germination results, on the induction of gene expression of all three genes following ABA treatment, *NRP-GFP* and *FyPP3/FyPP1 RNAi* were mildly more sensitive to ABA than the WT, whereas *nrp* and *FyPP3-RFP* were more resistant (Figure 6C–6E and Supplemental Figure 6). The mutual neutralizing effect between NRP and FyPP3 could be seen clearly in the results from the double transgenic lines. Overexpression of FyPP3 on *nrp* led to a reduced response to ABA compared with *FyPP3-RFP* or *nrp* alone, and the

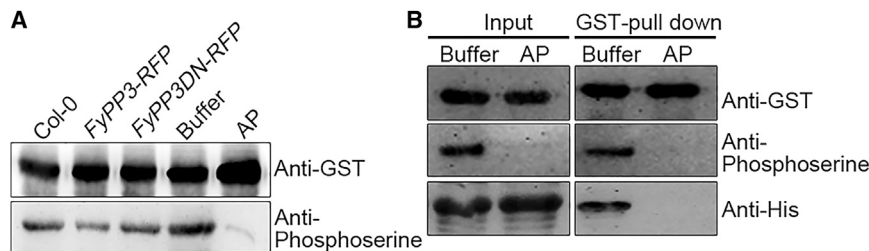


Figure 5. Dephosphorylation of NRP by FyPP3.

(A) *In vitro* dephosphorylation of NRP. Prokaryotically expressed/purified GST-DCD^{NRP} was incubated with homogenates of the WT (Col-0), *FyPP3-RFP*, and *FyPP3DN-RFP*, and the amount of total GST-DCD^{NRP} and phospho-DCD^{NRP} were detected by anti-GST and anti-phosphoserine antibodies, respectively. GST-DCD^{NRP} treated with buffer or alkaline phosphatase (AP) was used as controls.

(B) Dephosphorylated NRP no longer interact with FyPP3. Same amount of GST-DCD^{NRP} was treated with buffer or AP before GST pull-down and 6×His-MBP-FyPP3 detection. Anti-GST, anti-phosphoserine, and anti-6×His antibodies were used for immunoblotting.

FyPP3-RFP NRP-GFP line was similar to the WT (Figure 6C–6E and Supplemental Figure 6). These results indicated that the NRP–FyPP3 is an integral part of the ABA signaling network.

The negative role of FyPP3 in ABA signaling is achieved through its dephosphorylation and subsequent destabilization of the key transcription factor ABI5 (Dai et al., 2013). To find out whether NRP is also a part of this regulation, we carried out both genetic and biochemical analyses. Firstly, a transgenic line that overexpresses *ABI5*, *Pro35S:MYC-ABI5* (Bu et al., 2009), was crossed with *nrp*, and *nrp Pro35S:MYC-ABI5* was obtained and analyzed for its germination upon ABA treatment. The absence of NRP has little effect on the ABA-sensitive phenotype of *Pro35S:MYC-ABI5* (Figure 7A and 7B), indicating that NRP functions upstream of ABI5. It is also possible that the cellular concentration of ABI5 protein is sufficiently high when expressed under the 35S promoter, thus compensating for the hypophosphorylated state in the *nrp* background, masking the differences in the overall ABA sensitivities between *Pro35S:MYC-ABI5* and *nrp Pro35S:MYC-ABI5*. We then analyzed the ABA-induced turnover of ABI5 in the nine lines (Figure 7C). As reported, ABA stabilized ABI5 in the WT (Hu et al., 2014), whereas overexpression of *FyPP3* led to accelerated degradation of ABI5 (Dai et al., 2013). In *FyPP3 RNAi* or *DN* lines, ABI5 is also stabilized as reported (Dai et al., 2013). In *nrp*, ABI5 is rapidly degraded, and overexpression of *FyPP3* in the background of *nrp* further accelerated the turnover of ABI5. In contrast, overexpression of *NRP* stabilized ABI5. Finally, in the *FyPP3-RFP NRP-GFP* double transgenic line, degradation of ABI5 was attenuated compared with that in *FyPP3* overexpression alone. These observations indicated that the NRP–FyPP3 interaction likely acts upstream of ABI5 in the ABA signaling network.

DISCUSSION

In this study, we identified NRP as a new positive regulator in ABA signaling. We showed that NRP is able to interact with the PP6 catalytic subunit FyPP3 *in vitro* and *in vivo*, and can tether FyPP3 to SYP41/61-positive early endosomes *in vivo*. FyPP3, on the other hand, is able to dephosphorylate NRP *in vitro*, and the phosphorylation of NRP is a requisite for the NRP–FyPP3 interaction. ABA induces the expression of *NRP*, and promotes the vacuolar-dependent turnover of the two proteins. Genetic analyses confirmed that NRP is a positive regulator in ABA-mediated germination suppression, and biochemical evidence indicated that the NRP–FyPP3 circuit functions upstream of the

transcription factor ABI5 in ABA signaling. We propose a working model illustrating these findings in Figure 8.

NRP as a Positive Regulator in ABA Signaling

The DCD-domain-containing NRP proteins have been established as signal transducers in PCD elicited by pathogen infection, ER stress, and osmotic stress (Ludwig and Tenhaken, 2001; Costa et al., 2008). The downstream components of the DCD/NRP-mediated cell death signaling include the NAC (NAM, ATAF1/2, and CUC2)-domain-containing transcription factors and the vacuolar processing enzyme VPE (Hoepflinger et al., 2011; Reis et al., 2016). However, the molecular function of NRP is far from clear (Hoepflinger et al., 2011; Reis et al., 2016). To address this, we carried out a yeast two-hybrid screen and identified an important ABA signaling component, FyPP3, as an NRP-interacting partner, and further worked out the details on their interaction, intracellular distribution, and dynamics. We also showed that NRP may attenuate FyPP3-regulated ABI5 degradation, and thus positively regulate ABA signaling.

Eight different germplasm were obtained or generated to elucidate the NRP–FyPP3 signaling circuit. Among them, the *nrp* mutant is the same one used in all previous reports (Hoepflinger et al., 2011; Reis et al., 2016). For FyPP3 loss-of-function studies, we used both an RNAi line that targets both FyPP1 and FyPP3, and a DN line, with the latter used in previous studies on FyPP3 (Dai et al., 2012, 2013). To circumvent the auxin-related phenotypes observed in the severe RNAi lines (Dai et al., 2012), the lines used in this study had moderate ectopic expression levels and normal growth under controlled conditions (Supplemental Figure 1).

The NRP–FyPP3 signaling circuit turned out to be a complex one (Figure 8). We were intrigued to see their mutual suppression of each other's half-life especially following ABA treatment. In our working model, at the resting state the NRP protein level can be very low as it has a low mRNA level (Figure 3A) and a high turnover rate (Figure 3C). ABA can steadily induce the transcription of *NRP* (Figure 3A), and the half-life of NRP is prolonged (Figure 3C). The accumulated NRP can interact with FyPP3, which is rather stable in the absence of ABA, and tether it from the PM to TGN/EE (Figures 2 and 4). The fact that nearly 90% of FyPP3 puncta co-localize with NRP, whereas only a third of NRP co-localize with FyPP3, suggested that NRP may have other targets/functions in intracellular trafficking (Figure 2C and 2D), which can be ABA dependent or independent. The two interlocked proteins are likely targeted for vacuolar degradation, since the tonoplast proton pump inhibitor

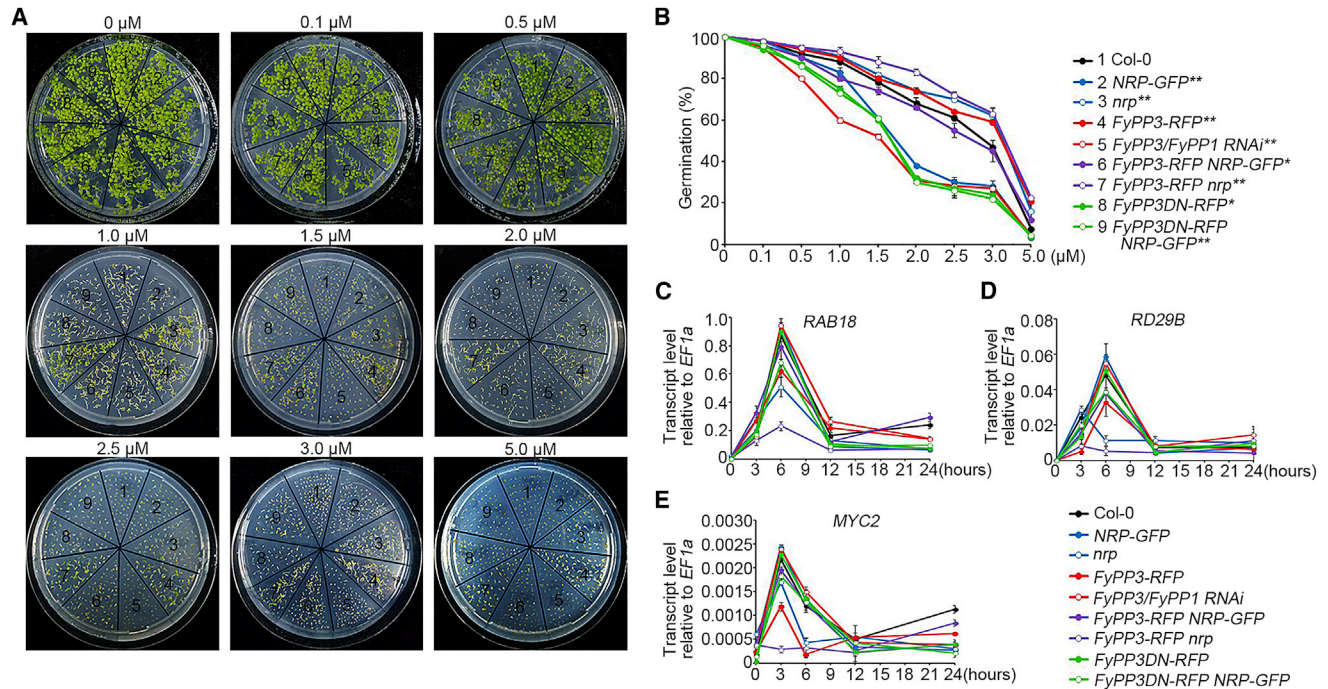


Figure 6. ABA Responses of Knockout and Transgenic Lines.

(A) Germination phenotypes of various knockout and transgenic lines on plates containing different concentrations of ABA. 1, Col-0; 2, *NRP-GFP*; 3, *nrp*; 4, *FyPP3-RFP*; 5, *FyPP3/FyPP1 RNAi*; 6, *FyPP3-RFP NRP-GFP*; 7, *FyPP3-RFP nrp*; 8, *FyPP3DN-RFP*; 9, *FyPP3DN-RFP NRP-GFP*. All transgenic lines were driven by 35S promoter.

(B) Quantification of (A). The germination rates were calculated from three independent experiments, with more than 150 seeds per line used for each experiment. The statistically significant differences between each line and Col-0 were calculated by Student's *t*-test: **p* < 0.05, ***p* < 0.01. Error bars denote SD.

(C–E) The transcript levels of ABA-responsive genes in various lines: (C) *RAB18*, (D) *RD29B*, and (E) *MYC2*. At least three biological replicates, each composed of four technical repeats, were performed for each gene. *EF1a* was used as an internal control. Error bars denote SD.

bafilomycin, instead of the 26S proteasome inhibitor MG132, attenuated the ABA-induced turnover of both proteins (Figure 3E and 3F). Such degradation can lead to the reduced level (and activity) of FyPP3 and the subsequent stabilization of ABI5 (Figure 7C), and eventually the ABA-induced transcription and germination inhibition (Figure 6).

We noticed that NRP is different from other known FyPP3 substrates, such as ABI5, PIN1, and PhyA (Kim et al., 2002; Dai et al., 2012, 2013), in that the NRP–FyPP3 circuit might be regulated bilaterally by NRP-mediated degradation and FyPP3-mediated dephosphorylation. As in the case of ABI5, there could be a kinase that phosphorylates NRP in the first place, or there could be one to antagonize FyPP3 activity once the interaction happens.

The Possible Roles for NRP in Integrating ABA Signaling and Other Pathways

The co-localization of NRP and SYP41/61 provided a clue for NRP in intracellular trafficking. Both SYP41 and SYP61 play roles in both endocytic and exocytic trafficking, and are included in a protein complex localized on the TGN (Drakakaki et al., 2012; Fuji et al., 2016). Previous research revealed that the regulation of ABA biosynthesis and vesicle trafficking under osmotic stress depends on the vacuolar sorting receptor 1 (VSR1). The loss of *VSR1* (*ced2* mutant) led to sensitivity toward ABA (Wang

et al., 2015). Additionally, the mutant line *osm1/syp61* showed impaired ABA-induced responses, such as stomata closure (Zhu et al., 2002). It has also been shown that ABI5 nuclear-cytoplasmic partitioning is regulated by its turnover through the E3 ligase KEG at the TGN/EE (Liu and Stone, 2013). Our study is in line with these reports in illuminating the importance of vesicle trafficking in ABA signaling.

In summary, our study adds NRP as a critical component to the FyPP3-mediated ABA signaling pathway. Considering that both proteins are involved in diverse physiological and pathological responses, further investigation is needed to elucidate their detailed roles in ABA and other signaling pathways in future.

METHODS

Generation of Transgenic Lines and Plant Growth Conditions

The NRP-related transgenic lines were generously provided by Dr. Raimund Tenhaken (University of Salzburg, Austria). For the *FyPP3-RFP* line, the *FyPP3-RFP* fusion gene was cloned to pCAMBIA1302 vector under the control of the 35S promoter and was introduced into the *Arabidopsis thaliana* ecotype Col-0 by floral dipping (Clough and Bent, 1998). *FyPP3/FyPP1 RNAi* lines were generated as described by Xu et al. (2010). For *FyPP3DN-RFP*, the D81N mutation was generated by site-directed mutagenesis (Stratagene, USA), and the transgenic plant was produced as for *FyPP3-RFP*. The double transgenic lines were generated by introducing *FyPP3* constructs into *nrp* or *NRP-GFP* transgenic plants. Transgenic plants were

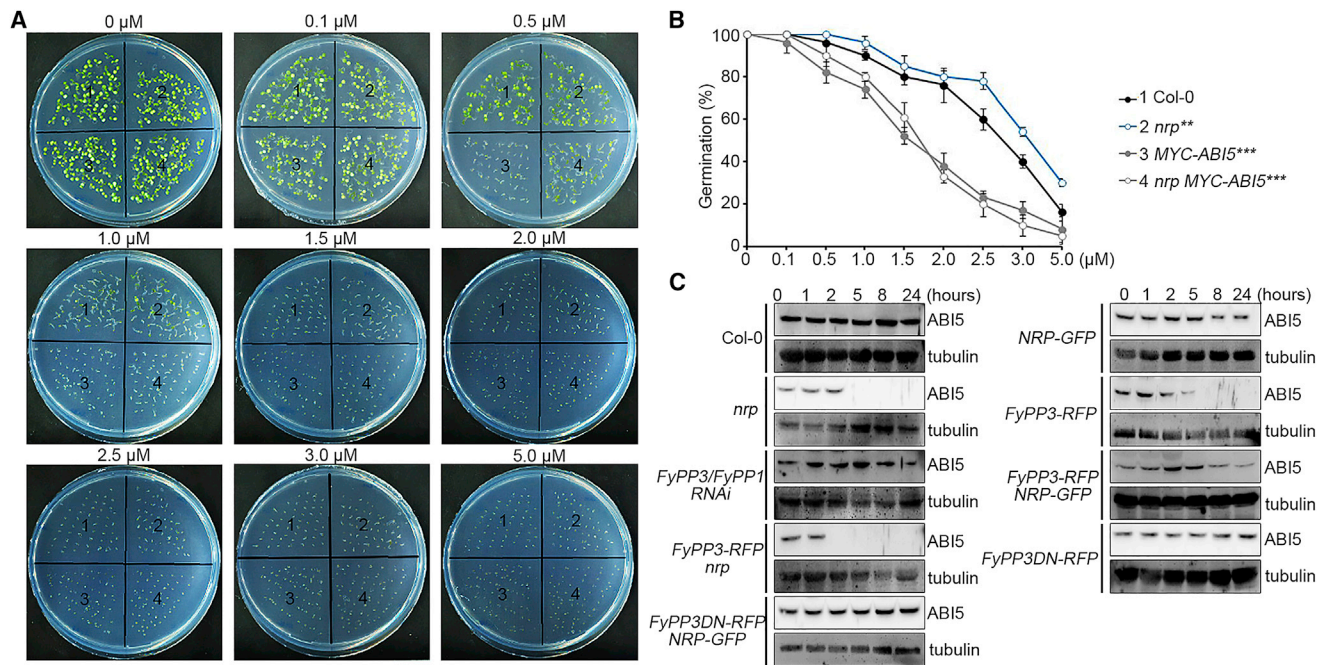


Figure 7. NRP and FyPP3 Act Upstream of ABI5.

(A) The germination rates of (1) Col-0, (2) *nrp*, (3) *MYC-ABI5*, and (4) *nrp MYC-ABI5*.

(B) Quantification of (A). The germination rates were calculated from three independent experiments, with more than 150 seeds per line used for each experiment. The statistically significant differences between each line and Col-0 were calculated by Student's *t*-test: ***p* < 0.01, ****p* < 0.001. Error bars denote SD.

(C) NRP attenuates FyPP3-mediated ABI5 degradation. Six-day-old seedlings were immersed in 5 μM ABA and collected at 0, 1, 2, 5, 8, and 24 h. Anti-ABI5 antibody was used for ABI5 detection. Tubulin was used as the loading control.

screened using 25 mg/l hygromycin or 0.1% glufosinate (BASTA). The seeds were harvested, surface sterilized in 75% ethanol, washed five times with ddH₂O, and kept at 4°C for 3 days for stratification before plating on half-strength Murashige and Skoog (1/2 MS) medium containing 1% sucrose. Seven-day-old seedlings were transplanted into soil for further growth at 22°C with an approximate irradiance of 110 $\mu\text{mol}/\text{m}^2/\text{s}$ for a 16-h day and 8-h night period.

For *ProNRP:GFP* and *ProFyPP3:GFP*, the full-length intergenic regions between *At5g42040* and *At5g42050* (*NRP*) and between *At3g19970* and *At3g19980* (*FyPP3*), representative of the promoters of *NRP* and *FYPP3*, respectively, were PCR-amplified and inserted into *pCAMBIA1302*. The constructs were introduced into *Agrobacterium tumefaciens* (GV3101) for floral dipping (Clough and Bent, 1998). Primary transformants were selected by hygromycin resistance. *Pro35S:MYC-ABI5* line, a gift from Dr. Jigang Li (China Agricultural University, China) (Bu et al., 2009), was introduced into *nrp* (*salk_041306*) by crossing, and *nrp MYC-ABI5* homozygotes were isolated from the F2 population.

All transgenic lines were verified with genomic PCR and RT-PCR, and T3/F3 homozygous lines were used for further analyses. The primers used are listed in Supplemental Table 2.

Yeast Two-Hybrid Assay

Yeast two-hybrid assay was carried out following the protocol of the Matchmaker Gold Yeast Two-Hybrid System (Clontech, USA). Matchmaker Pretransformed library (Universal Arabidopsis) was used for screening. NRP was used as the bait.

GST Pull-Down Assay

6 \times His-MBP-FyPP3 (or FyPP3DN) and GST-DCD^{NRP} were expressed separately in *E. coli*, and cell pellets were mixed for lysis by sonication.

Following centrifugation at 10 000 *g* for 20 min, the supernatant was incubated with glutathione Sepharose (GE Healthcare, USA). The beads were washed four times and the final proteins were eluted by 10 mM reduced glutathione (GSH). The collected proteins were used for western blotting. The anti-6 \times His antibody was used to detect the binding FyPP3 and FyPP3DN.

For the GST pull-down between dephosphorylated NRP and FyPP3, GST-DCD^{NRP} was firstly treated by AP or Thermo Scientific FastAP reaction buffer prior to GST pull-down. Anti-GST, anti-phosphoserine, and anti-6 \times His antibodies were used for immunoblotting.

Bimolecular Fluorescence Complementation Assay

The NRP coding sequence was cloned into *pSPYNE173* vector (NRP-nEYFP), and FyPP3 was cloned into *pSPYCE(M)* vector (FyPP3-cEYFP). These constructs were introduced into *A. tumefaciens* strain GV3101. Leaves from 5-week-old tobacco (*Nicotiana benthamiana*) plants were inoculated with transformed agrobacteria as described by Xiong et al. (2016). Fluorescence generated by protein interaction was visualized under a Leica TCS SP8 confocal microscope at a wavelength of 550 nm.

Antibody Production

6 \times His-tagged NRP was expressed in *E. coli*, purified under denaturing condition with Ni-nitrilotriacetic acid resin (GE Healthcare) in 8 M urea, 50 mM Tris-HCl (pH 7.5), and refolded by dilution. 6 \times His-MBP-FyPP3 was expressed and purified with amylose resin (GE Healthcare, USA) and the tag was removed subsequently by tobacco etch virus protease. Antibodies were then generated from parallel immunizations of rabbits.

Laser Scanning Confocal Microscopy

GFP- or RFP-tagged *NRP* and *FyPP3*, the endosomal markers *SYP41*, *SYP61*, and *Fab1A*, and the PM marker *PIP2;1* were cloned into

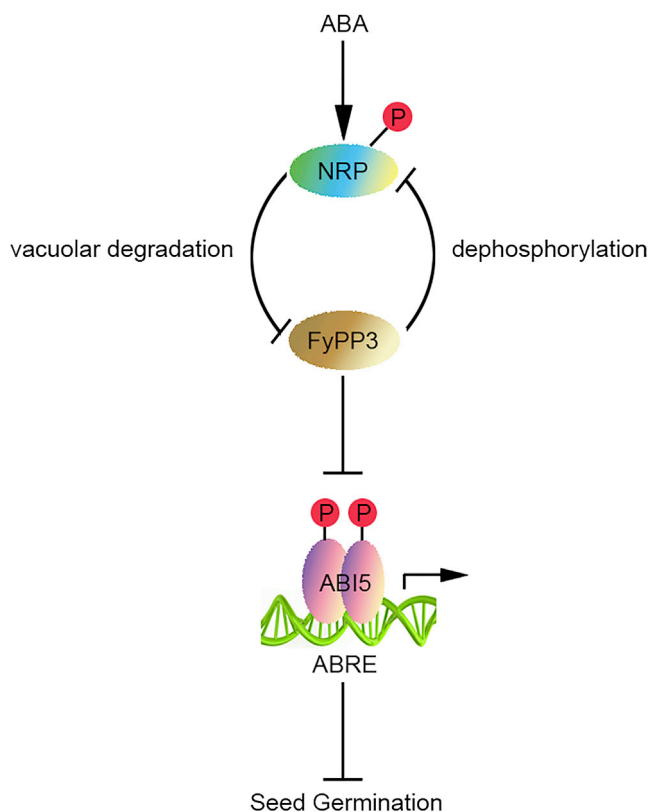


Figure 8. The Working Model.

ABA induces *NRP* expression, and *NRP* facilitates *FyPP3* degradation to stabilize *ABI5* *in vivo*. Meanwhile, *FyPP3* is able to dephosphorylate *NRP* *in vitro*.

pCAMBIA1302, verified by DNA sequencing, and introduced into *A. tumefaciens* (GV3101) for transient expression in tobacco leaves as described by Xiong et al. (2016). After 2 days of inoculation the leaves were collected and lower leaf epidermis was peeled off, incubated in 5% glycerol, and scanned with a Leica TCS SP8 (Leica, Germany) as described by Xiong et al. (2016).

Degradation Assay of *NRP*, *FyPP3*, and *ABI5*

For detection of the degradation of *NRP*, the lines *NRP-GFP*, *FyPP3-RFP*, *NRP-GFP*, and *FyPP3DN-RFP* *NRP-GFP* were cultivated for 7 days and immersed in 1 mg/l cycloheximide (CHX) for 5.5 h. The seedlings were immersed in the solution with or without 2 μ M ABA. The roots were then harvested at different time points following CHX removal. The samples were homogenized with protein extraction buffer (50 mM Tris-HCl [pH 7.5], 10 mM MgCl₂, 150 mM NaCl, 0.5% Triton X-100, 1 mM PMSF, 2% β -mercaptoethanol) and prepared for further western blotting with GFP antibody and tubulin antibody. To detect the degradation of *FyPP3*, we immersed 7-day-old *FyPP3-RFP*, *FyPP3-RFP* *NRP-GFP*, and *FyPP3-RFP* *nrp* seedlings in 1 mg/l CHX for 15 h. ABA (2 μ M) was added prior to the harvesting of seedlings. For the degradation inhibition assay, 20 μ M MG132 or 40 nM bafilomycin were additionally added. Anti-RFP and anti-tubulin antibodies were used for immunoblotting. Anti-*ABI5* antibody was obtained from Abcam (UK).

In Vitro Dephosphorylation Assay

GST-DCD^{NRP} was expressed and purified from *E. coli*. Purified protein was divided into five aliquots and incubated with the homogenates of Col-0, *FyPP3-RFP*, *FyPP3DN-RFP*, kinase/phosphatase buffer, or AP for 30 min at 30°C, respectively. The kinase/phosphatase buffer used in this work was prepared following a previous work (Dai et al., 2013).

Germination Assay

Arabidopsis seeds were planted on 1/2 MS medium plates containing different concentrations of ABA. Germination percentage (radicle emergence) was scored on day 7 as described by Ren et al. (2016).

Gene Expression Analysis

RNA extraction, reverse transcription, RT-PCR, and qRT-PCR were performed as described by Xiong et al. (2016). Primers used are listed in Supplemental Table 2.

ACCESSION NUMBERS

The accession numbers of genes mentioned in this study in the Arabidopsis Genome Initiative database are as follows: *FyPP3* (AT3G19980), *FyPP1* (AT1G50370), *NRP* (AT5G42050), *SnRK2* (AT1G10940), *ABI5* (AT2G36270), *RCN1* (AT1G25490), *SYP41* (AT5G26980), *SYP61* (AT1G28490), *PIP2;1* (AT3G53420), *FAB1a* (AT4G33240), *RD29B* (AT5G52300), *RAB18* (AT5G66400), *MYC2* (AT1G32640), *EF1a* (AT5G60390), *TIP4;1-like* (AT4G34270), and *AP2M* (AT5G46630).

SUPPLEMENTAL INFORMATION

Supplemental Information is available at *Molecular Plant Online*.

FUNDING

X.L. is supported by the National Key Research and Development Plan (2017YFD0200900), National Natural Science Foundation of China (31370925 and 31640024). Q.G. is supported by the National Natural Science Foundation of China (31401179 and 31671419).

AUTHOR CONTRIBUTIONS

X.L. and Q.G. conceived the project and designed the experiments. T.Z., Y.W., X.Y., and W.C. performed the experiments. T.Z., X.L., and Q.G. analyzed the data. X.L. and Q.G. wrote the paper.

ACKNOWLEDGMENTS

We thank Drs. Raimund Tenhaken (University of Salzburg, Austria), Jigang Li (China Agricultural University, China), Chuanyou Li (Institute of Genetics and Developmental Biology, Chinese Academy of Sciences, China), and Mingqiu Dai (Huazhong Agricultural University, China) for providing *NRP* and *ABI5* related transgenic seeds. No conflict of interest declared.

Received: October 26, 2017

Revised: October 26, 2017

Accepted: November 14, 2017

Published: November 23, 2017

REFERENCES

- Albertos, P., Romero-Puertas, M.C., Tatematsu, K., Mateos, I., Sanchez-Vicente, I., Nambara, E., and Lorenzo, O. (2015). S-nitrosylation triggers *ABI5* degradation to promote seed germination and seedling growth. *Nat. Commun.* 6:10.
- Bauer, H., Ache, P., Lautner, S., Fromm, J., Hartung, W., Al-Rasheid, K.A.S., Sonnewald, S., Sonnewald, U., Kneitz, S., Lachmann, N., et al. (2013). The stomatal response to reduced relative humidity requires guard cell-autonomous ABA synthesis. *Curr. Biol.* 23:53–57.
- Belda-Palazon, B., Rodriguez, L., Fernandez, M.A., Castillo, M.C., Anderson, E.A., Gao, C., Gonzalez-Guzman, M., Peirats-Llobet, M., Zhao, Q., De Winne, N., et al. (2016). FYVE1/FREE1 interacts with the PYL4 ABA receptor and mediates its delivery to the vacuolar degradation pathway. *Plant Cell* <https://doi.org/10.1105/tpc.16.00178>.
- Bensmihen, S., Ripa, S., Lambert, G., Jublot, D., Pautot, V., Granier, F., Giraudat, J., and Parcy, F. (2002). The homologous *ABI5* and *EEL* transcription factors function antagonistically to fine-tune gene expression during late embryogenesis. *Plant Cell* 14:1391–1403.

- Brocard, I.M., Lynch, T.J., and Finkelstein, R.R.** (2002). Regulation and role of the *Arabidopsis* Abscisic Acid-Insensitive 5 gene in abscisic acid, sugar, and stress response. *Plant Physiol.* **129**:1533–1543.
- Bu, Q., Li, H., Zhao, Q., Jiang, H., Zhai, Q., Zhang, J., Wu, X., Sun, J., Xie, Q., Wang, D., et al.** (2009). The *Arabidopsis* RING finger E3 ligase RHA2a is a novel positive regulator of abscisic acid signaling during seed germination and early seedling development. *Plant Physiol.* **150**:463–481.
- Carles, C., Bies-Etheve, N., Aspart, L., Leon-Kloosterziel, K.M., Koornneef, M., Echeverria, M., and Delseny, M.** (2002). Regulation of *Arabidopsis thaliana* Em genes: role of ABI5. *Plant J.* **30**:373–383.
- Chiwocha, S.D.S., Cutler, A.J., Abrams, S.R., Ambrose, S.J., Yang, J., Ross, A.R.S., and Kermod, A.R.** (2005). The *etr1-2* mutation in *Arabidopsis thaliana* affects the abscisic acid, auxin, cytokinin and gibberellin metabolic pathways during maintenance of seed dormancy, moist-chilling and germination. *Plant J.* **42**:35–48.
- Clough, S.J., and Bent, A.F.** (1998). Floral dip: a simplified method for *Agrobacterium*-mediated transformation of *Arabidopsis thaliana*. *Plant J.* **16**:735–743.
- Costa, M.D.L., Reis, P.A.B., Valente, M.A.S., Irsigler, A.S.T., Carvalho, C.M., Loureiro, M.E., Aragao, F.J.L., Boston, R.S., Fietto, L.G., and Fontes, E.P.B.** (2008). A new branch of endoplasmic reticulum stress signaling and the osmotic signal converge on plant-specific asparagine-rich proteins to promote cell death. *J. Biol. Chem.* **283**:20209–20219.
- Cutler, S.R., Rodriguez, P.L., Finkelstein, R.R., and Abrams, S.R.** (2010). Abscisic acid: emergence of a core signaling network. *Annu. Rev. Plant Biol.* **61**:651–679.
- Dai, M.Q., Zhang, C., Kania, U., Chen, F., Xue, Q., McCray, T., Li, G., Qin, G.J., Wakeley, M., Terzaghi, W., et al.** (2012). A PP6-type phosphatase holoenzyme directly regulates pin phosphorylation and auxin efflux in *Arabidopsis*. *Plant Cell* **24**:2497–2514.
- Dai, M.Q., Xue, Q., McCray, T., Margavage, K., Chen, F., Lee, J.H., Nezames, C.D., Guo, L.Q., Terzaghi, W., Wan, J.M., et al.** (2013). The PP6 phosphatase regulates ABI5 phosphorylation and abscisic acid signaling in *Arabidopsis*. *Plant Cell* **25**:517–534.
- Drakakaki, G., van de Ven, W., Pan, S.Q., Miao, Y.S., Wang, J.Q., Keinath, N.F., Weatherly, B., Jiang, L.W., Schumacher, K., Hicks, G., et al.** (2012). Isolation and proteomic analysis of the SYP61 compartment reveal its role in exocytic trafficking in *Arabidopsis*. *Cell Res.* **22**:413–424.
- Endo, A., Sawada, Y., Takahashi, H., Okamoto, M., Ikegami, K., Koiwai, H., Seo, M., Toyomasu, T., Mitsuhashi, W., Shinozaki, K., et al.** (2008). Drought induction of *Arabidopsis* 9-cis-epoxycarotenoid dioxygenase occurs in vascular parenchyma cells. *Plant Physiol.* **147**:1984–1993.
- Finkelstein, R.R.** (2006). Studies of abscisic acid perception finally flower. *Plant Cell* **18**:786–791.
- Finkelstein, R.** (2013). Abscisic acid synthesis and response. *Arabidopsis Book* **11**:e0166.
- Finkelstein, R., Gampala, S.S.L., Lynch, T.J., Thomas, T.L., and Rock, C.D.** (2005). Redundant and distinct functions of the ABA response loci ABA-INSENSITIVE(ABI)5 and ABRE-BINDING FACTOR (ABF)3. *Plant Mol. Biol.* **59**:253–267.
- Finkelstein, R., Reeves, W., Ariizumi, T., and Steber, C.** (2008). Molecular aspects of seed dormancy. *Annu. Rev. Plant Biol.* **59**:387–415.
- Finkelstein, R.R., and Lynch, T.J.** (2000). The *Arabidopsis* abscisic acid response gene ABI5 encodes a basic leucine zipper transcription factor. *Plant Cell* **12**:599–609.
- Fuji, K., Shirakawa, M., Shimono, Y., Kunieda, T., Fukao, Y., Koumoto, Y., Takahashi, H., Hara-Nishimura, I., and Shimada, T.** (2016). The adaptor complex AP-4 regulates vacuolar protein sorting at the trans-Golgi network by interacting with VACUOLAR SORTING RECEPTOR1. *Plant Physiol.* **170**:211–219.
- Fujita, Y., Fujita, M., Shinozaki, K., and Yamaguchi-Shinozaki, K.** (2011). ABA-mediated transcriptional regulation in response to osmotic stress in plants. *J. Plant Res.* **124**:509–525.
- Furihata, T., Maruyama, K., Fujita, Y., Umezawa, T., Yoshida, R., Shinozaki, K., and Yamaguchi-Shinozaki, K.** (2006). Abscisic acid-dependent multisite phosphorylation regulates the activity of a transcription activator AREB1. *Proc. Natl. Acad. Sci. USA* **103**:1988–1993.
- Hauser, F., Waadt, R., and Schroeder, J.I.** (2011). Evolution of abscisic acid synthesis and signaling mechanisms. *Curr. Biol.* **21**:R346–R355.
- Hoepflinger, M.C., Pieslinger, A.M., and Tenhaken, R.** (2011). Investigations on N-rich protein (NRP) of *Arabidopsis thaliana* under different stress conditions. *Plant Physiol. Biochem.* **49**:293–302.
- Hu, R., Zhu, Y., Shen, G., and Zhang, H.** (2014). TAP46 plays a positive role in the ABSCISIC ACID INSENSITIVE5-regulated gene expression in *Arabidopsis*. *Plant Physiol.* **164**:721–734.
- Kim, D.H., Kang, J.G., Yang, S.S., Chung, K.S., Song, P.S., and Park, C.M.** (2002). A phytochrome-associated protein phosphatase 2A modulates light signals in flowering time control in *Arabidopsis*. *Plant Cell* **14**:3043–3056.
- Lee, J.H., Yoon, H.J., Terzaghi, W., Martinez, C., Dai, M.Q., Li, J.G., Byun, M.O., and Deng, X.W.** (2010). DWA1 and DWA2, two *Arabidopsis* DWD protein components of CUL4-based E3 ligases, act together as negative regulators in ABA signal transduction. *Plant Cell* **22**:1716–1732.
- Lee, K.P., Piskurewicz, U., Tureckova, V., Carat, S., Chappuis, R., Strnad, M., Fankhauser, C., and Lopez-Molina, L.** (2012). Spatially and genetically distinct control of seed germination by phytochromes A and B. *Genes Dev.* **26**:1984–1996.
- Liu, H.X., and Stone, S.L.** (2010). Abscisic acid increases *Arabidopsis* ABI5 transcription factor levels by promoting KEG E3 ligase self-ubiquitination and proteasomal degradation. *Plant Cell* **22**:2630–2641.
- Liu, H.X., and Stone, S.L.** (2013). Cytoplasmic degradation of the *Arabidopsis* transcription factor ABSCISIC ACID INSENSITIVE 5 is mediated by the RING-type E3 ligase KEEP on GOING. *J. Biol. Chem.* **288**:20267–20279.
- Lopez-Molina, L., Mongrand, S., and Chua, N.H.** (2001). A postgermination developmental arrest checkpoint is mediated by abscisic acid and requires the ABI5 transcription factor in *Arabidopsis*. *Proc. Natl. Acad. Sci. USA* **98**:4782–4787.
- Ludwig, A.A., and Tenhaken, R.** (2001). A new cell wall located n-rich protein is strongly induced during the hypersensitive response in *Glycine max* L. *Eur. J. Plant Pathol.* **107**:323–336.
- Ma, Y., Szostkiewicz, I., Korte, A., Moes, D., Yang, Y., Christmann, A., and Grill, E.** (2009). Regulators of PP2C phosphatase activity function as abscisic acid sensors. *Science* **324**:1064–1068.
- Miura, K., Lee, J., Jin, J.B., Yoo, C.Y., Miura, T., and Hasegawa, P.M.** (2009). Sumoylation of ABI5 by the *Arabidopsis* SUMO E3 ligase SIZ1 negatively regulates abscisic acid signaling. *Proc. Natl. Acad. Sci. USA* **106**:5418–5423.
- Nakashima, K., Fujita, Y., Kanamori, N., Katagiri, T., Umezawa, T., Kidokoro, S., Maruyama, K., Yoshida, T., Ishiyama, K., Kobayashi, M., et al.** (2009). Three *Arabidopsis* SnRK2 protein kinases, SRK2D/SnRK2.2, SRK2E/SnRK2.6/OST1 and SRK2I/SnRK2.3, involved in ABA signaling are essential for the control of seed development and dormancy. *Plant Cell Physiol.* **50**:1345–1363.
- Park, S.Y., Fung, P., Nishimura, N., Jensen, D.R., Fujii, H., Zhao, Y., Lumba, S., Santiago, J., Rodrigues, A., Chow, T.F.F., et al.** (2009).

- Abcisic acid inhibits type 2C protein phosphatases via the PYR/PYL family of START proteins. *Science* **324**:1068–1071.
- Qin, F., Shinozaki, K., and Yamaguchi-Shinozaki, K.** (2011). Achievements and challenges in understanding plant abiotic stress responses and tolerance. *Plant Cell Physiol.* **52**:1569–1582.
- Reis, P.A.A., Rosado, G.L., Silva, L.A.C., Oliveira, L.C., Oliveira, L.B., Costa, M.D.L., Alvim, F.C., and Fontes, E.P.B.** (2011). The binding protein BiP attenuates stress-induced cell death in soybean via modulation of the N-rich protein-mediated signaling pathway. *Plant Physiol.* **157**:1853–1865.
- Reis, P.A.B., Carpinetti, P.A., Freitas, P.P.J., Santos, E.G.D., Camargos, L.F., Oliveira, I.H.T., Silva, J.C.F., Carvalho, H.H., Dal-Bianco, M., Soares-Ramos, J.R.L., et al.** (2016). Functional and regulatory conservation of the soybean ER stress-induced DCD/NRP-mediated cell death signaling in plants. *BMC Plant Biol.* **16**:19.
- Ren, C., Zhu, X., Zhang, P., and Gong, Q.** (2016). *Arabidopsis* COP1-interacting protein 1 is a positive regulator of ABA response. *Biochem. Biophys. Res. Commun.* **477**:847–853.
- Rodriguez, L., Gonzalez-Guzman, M., Diaz, M., Rodrigues, A., Izquierdo-Garcia, A.C., Peirats-Llobet, M., Fernandez, M.A., Antoni, R., Fernandez, D., Marquez, J.A., et al.** (2014). C2-domain abscisic acid-related proteins mediate the interaction of PYR/PYL/RCAR abscisic acid receptors with the plasma membrane and regulate abscisic acid sensitivity in *Arabidopsis*. *Plant Cell* **26**:4802–4820.
- Sanderfoot, A.A., Kovaleva, V., Bassham, D.C., and Raikhel, N.V.** (2001). Interactions between syntaxins identify at least five SNARE complexes within the Golgi/prevacuolar system of the *Arabidopsis* cell. *Mol. Biol. Cell* **12**:3733–3743.
- Stone, S.L., Williams, L.A., Farmer, L.M., Vierstra, R.D., and Callis, J.** (2006). KEEP ON GOING, a RING E3 ligase essential for *Arabidopsis* growth and development, is involved in abscisic acid signaling. *Plant Cell* **18**:3415–3428.
- Tenhaken, R., Doerks, T., and Bork, P.** (2005). DCD—a novel plant specific domain in proteins involved in development and programmed cell death. *BMC Bioinformatics* **6**:169.
- Umezawa, T., Nakashima, K., Miyakawa, T., Kuromori, T., Tanokura, M., Shinozaki, K., and Yamaguchi-Shinozaki, K.** (2010). Molecular basis of the core regulatory network in ABA responses: sensing, signaling and transport. *Plant Cell Physiol.* **51**:1821–1839.
- Wang, Z.Y., Gehring, C., Zhu, J.H., Li, F.M., Zhu, J.K., and Xiong, L.M.** (2015). The *Arabidopsis* vacuolar sorting receptor1 is required for osmotic stress-induced abscisic acid biosynthesis. *Plant Physiol.* **167**:137–152.
- Xiong, J., Cui, X., Yuan, X., Yu, X., Sun, J., and Gong, Q.** (2016). The Hippo/STE20 homolog SIK1 interacts with MOB1 to regulate cell proliferation and cell expansion in *Arabidopsis*. *J. Exp. Bot.* **67**:1461–1475.
- Xu, G., Sui, N., Tang, Y., Xie, K., Lai, Y., and Liu, Y.** (2010). One-step, zero-background ligation-independent cloning intron-containing hairpin RNA constructs for RNAi in plants. *New Phytol.* **187**:240–250.
- Yu, F.F., Wu, Y.R., and Xie, Q.** (2015). Precise protein post-translational modifications modulate ABI5 activity. *Trends Plant Sci.* **20**:569–575.
- Yu, F., Lou, L., Tian, M., Li, Q., Ding, Y., Cao, X., Wu, Y., Belda-Palazon, B., Rodriguez, P.L., Yang, S., et al.** (2016). ESCRT-I component VPS23A affects ABA signaling by recognizing ABA receptors for endosomal degradation. *Mol. Plant* **9**:1570–1582.
- Zhu, J.H., Gong, Z.Z., Zhang, C.Q., Song, C.P., Damsz, B., Inan, G., Koiwa, H., Zhu, J.K., Hasegawa, P.M., and Bressan, R.A.** (2002). OSM1/SYP61: a syntaxin protein in *Arabidopsis* controls abscisic acid-mediated and non-abscisic acid-mediated responses to abiotic stress. *Plant Cell* **14**:3009–3028.